Spectral emissivity and temperature maps of the Solfatara crater from DAIS hyperspectral images

Luca Merucci ([1]), **Maria Paola Bogliolo** ([2]), **Maria Fabrizia Buongiorno** ([1]) **and Sergio Teggi** ([3])

([1]) *Istituto Nazionale di Geofisica e Vulcanologia, Roma, Italy*
([2]) *Istituto Superiore per la Prevenzione e la Sicurezza del Lavoro, Monteporzio Catone (RM), Italy*
([3]) *Università di Modena e Reggio Emilia, Modena, Italy*

Abstract
Quantitative maps of surface temperature and spectral emissivity have been retrieved on the Solfatara crater at Pozzuoli (Naples) from remote sensing hyperspectral data. The present study relies on thermal infrared images collected on July 27, 1997 by the DAIS hyperspectral sensor owned by the German aerospace center (DLR). The Emissivity Spectrum Normalization method was used to make temperature and emissivity estimates. Raw data were previously transformed in radiance and corrected for the atmospheric contributions using the MODTRAN radiative transfer code and the sensor response functions. During the DAIS flight a radiosonde was launched to collect the atmospheric profiles of pressure, temperature and humidity used as input to the code. Retrieved temperature values are in good agreement with temperature measurements performed *in situ* during the campaign. The spectral emissivity map was used to classify the image in different geo-mineralogical units with the Spectral Angle Mapper method. Areas of geologic interest were previously selected using a mask obtained from an NDVI image calculated with two channels of the visible (red) and the near infrared respectively.

Key words *hyperspectral data – surface temperature – spectral emissivity – Solfatara (Phlegraean Fields) – DAIS*

1. Introduction

Surface temperature and spectral emissivity of materials are valuable parameters in volcanology since they provide information on several aspects of the current activity and of past events. Mapping surface temperature allows us to estimate the heath flux from the surface and therefore to control activity inside vents and fractures. Spectral emissivity in the thermal infrared is a physical parameter necessary to calculate temperature, and moreover it enables recognition of surface materials on the basis of their spectral pattern (Salisbury and D'Aria, 1992); it is particularly suitable to study volcanic materials because the main absorption bands of silicates are located in the thermal infrared (Gillespie, 1985). Remote separation and identification of surface deposits in volcanic areas is useful to map lava flows on the basis of their composition, to characterize surface alteration due to hydrothermal phenomena and to identify newly formed deposits related to fumarolic activity.

Surface kinetic temperature and emissivity properties of materials can be estimated with high accuracy by remote sensing if images collected on several channels in the thermal infrared are available. Thermal infrared multi-channel sensors have been operating for a long time at low spatial resolution (less than one km, mainly for meteorologi-

Table I. DAIS 7915 main technical and spectral characteristics.

Spectrometer	Spectral region	No. of channels	Wavelength
1	0.4-1.0 μm	32	15-30 nm
2	1.5-1.8 μm	8	45 nm
3	2.0-2.5 μm	32	20 nm
	3.0-5.0 μm	1	2.0 μm
4	8.0-12.6 μm	6	0.9 μm

Dynamic range	15 bit
Ground resolution	5-20 m (function of the flight altitude)
Scan line dimension	512 pixels

Fig. 1. Topographic map of the Solfatara crater. Gray squares indicate the surface temperature measurement sites; the black circle (RS) locates the radiosonde launch site.

cal or oceanographic use), and only few instruments provide multi-channel images at high spatial resolution in this spectral range. The airborne hyperspectral sensors TIMS (NASA), MIVIS (CNR-LARA Project) and DAIS (German aerospace center DLR: http://www.op.dlr.de/dais/) and the spaceborne sensor ASTER onboard TERRA and AQUA satellites (NASA) are examples of this kind of instruments.

With the aim of understanding the capabilities of the DAIS (Digital Airborne Imaging Spectrometer) hyperspectral sensor to provide information of volcanological interest, we analyzed the thermal infrared DAIS data of an active volcanic area, according to three work phases: 1) retrieval of the radiance emitted by the surface, through atmospheric modeling; 2) estimation of surface temperature and spectral emissivity; 3) application of spectral mapping techniques to produce a thematic map of the main surface units.

2. Data set

Remote sensing data used in this study were provided by the DAIS 7915 spectrometer owned by the German aerospace center (DLR). The main spectral and technical characteristics of DAIS are summarized in table I. The image under investigation was collected on July 27, 1997 at 10:27 (local time) on the Solfatara crater at Pozzuoli (Naples, Italy) in the framework of the E.C. Large Scale Facilities Project, and under request and supervision of the Remote Sensing Laboratory of the Italian National Institute of Geophysics and Volcanology (INGV) of Rome. DAIS was flown on a DO 228 aircraft at an altitude of 1600 m a.s.l., and the collected images ground resolution is about 5 m. The data spectral subset used here corresponds to the six DAIS infrared thermal channels.

Simultaneously with the DAIS flight, a ground measurement campaign was carried out to measure the parameters necessary to atmospheric correction and validation of the retrieved maps. Vertical atmospheric profiles of pressure, temperature and relative humidity at about 10 m vertical resolution were measured by means of a radiosonde launch performed near the Solfatara (fig. 1).

Surface brightness temperature was measured with an infrared thermometer (EVEREST Inters. Inc.) at different sites (fig. 1), selected on homogeneous and horizontal surfaces easy to locate on the images. In order to compensate for the spatial scale difference between the ground measures and the remote sensing data, 10 measurements were acquired on different points at each site: the average value was considered to be representative of the site brightness temperature. Temperature inside fumaroles was also measured with a thermocouple.

3. Geological setting

Solfatara is a volcanic crater located in the central area of the Phlegraean Fields caldera complex, west of the city of Naples (Italy) (figs. 2, 3). It represents the most active zone of Phlegraean Fields, and sits inside the sprawling urban area of Pozzuoli.

Activity in the Phlegraean area has been dominated by two eruptions that produced widespread ash-flow deposits: the Campanian Ignimbrite and the smaller Neapolitan Yellow Tuff (Lirer *et al.*, 1987; Scandone *et al.*, 1991). The eruption producing the Campanian Ignimbrite occurred 37000 years BP and resulted in the collapse of a large area including Campi Flegrei and part of the gulf of Naples. The eruption of Neapolitan Yellow Tuff occurred 12000 years BP, had a very complex history that led to the formation of a caldera of smaller dimensions inside that of the Campanian Ignimbrite. In the last 12000 years, the bottom of the Neapolitan Yellow Tuff caldera has been the site of intense volcanic activity and ground deformation (Di Vito *et al.*, 1999). Volcanism was concentrated in three periods: 12000 and 9500 years BP, 8600 and 8200 years BP, and 4800 and 3800 years BP (*e.g.*, at Cigliano, Agnano-Monte Spina, Astroni, Averno, Solfatara), followed by the last eruption in 1538 that led to the formation of the Monte Nuovo (Di Vito *et al.*, 1987).

Since 1800, sea-level measurements made at ancient roman ruins have indicated a slow sinking of the area. This slow sinking of the ground continued until 1968. In the periods 1970-1972 and 1982-1984 two important bradyseismic
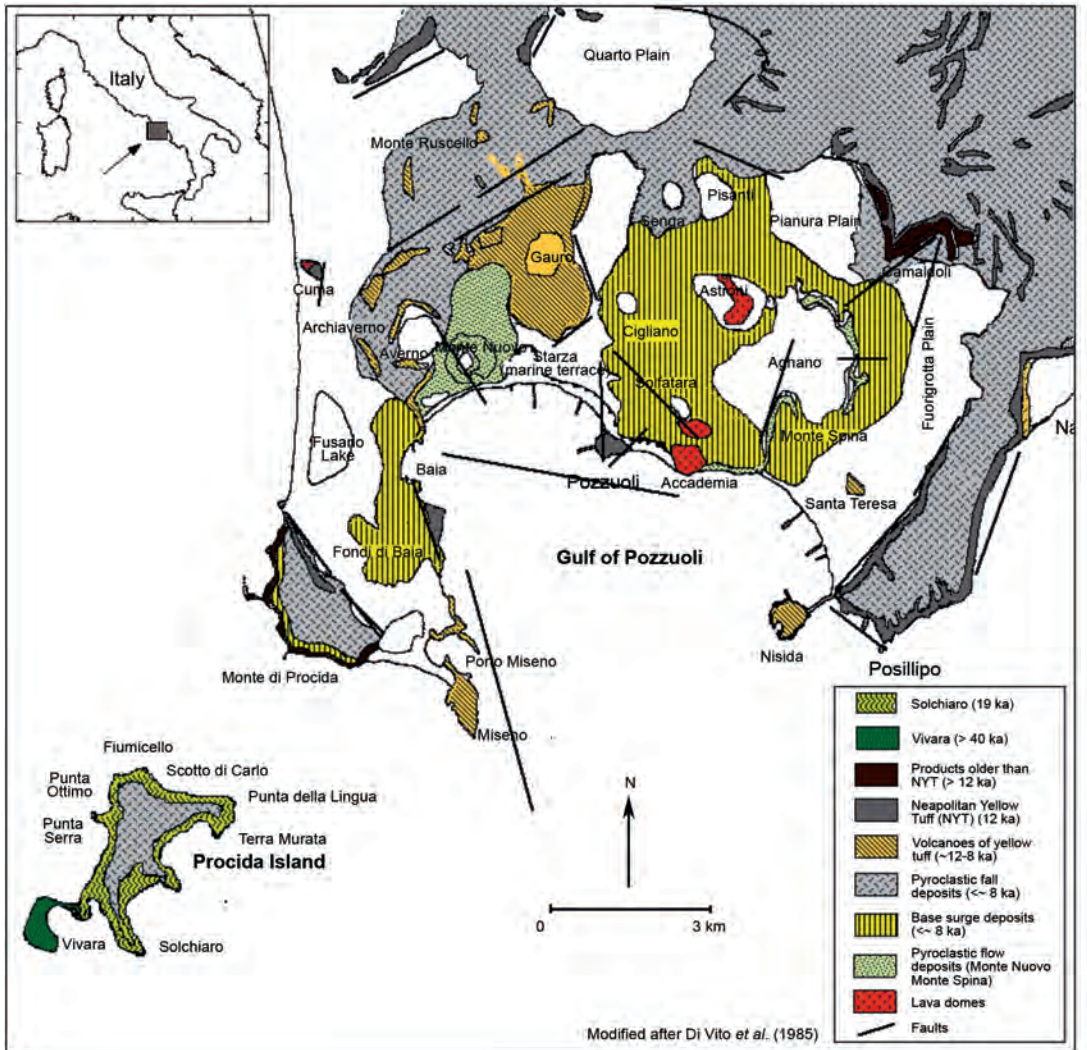
Fig. 2. Schematic geological map of the Phlegraean Fields (Scandone, 1997).

events (ground uplift) occurred in the Pozzuoli area (Corrado *et al.*, 1976; Berrino *et al.*, 1984), (maximum uplift of 1.7 and 1.8 m respectively) accompanied by shallow seismicity. More recently, two minor sudden ground uplifts and seismic swarms were recorded in 1989-1990 and in 1994.

The Solfatara volcano is one of the most recent (about 4000 years BP) of the Phlegraean Fields caldera. It measures 0.5×0.6 km, with steep walls on the north, east and south sides. To the west the crater wall is missing. Its rectangular shape is mostly due to the presence of faults at NW-SE and SW-NE. The volcanic cone is made of pyroclastic rocks, with the exception of Mt. Olibano that is a dome of trachytic lava.

The flat-floored crater (Piano Sterile) is characterized by strong fumarolic activity which

Fig. 3. Solfatara crater at Pozzuoli (Naples, Italy). Picture from «Pozzuoli dal cielo» by Aeromap Data.

causes both single vent emissions, with temperature up to 160°C, and diffuse degassing. The gases emitted are mostly composed by H_2O, CO_2, H_2S and smaller quantities of H_2, CH_4, He, HCl, Ar (Valentino *et al.*, 1999).

One of the most recent hydrothermal models (Chiodini *et al.*, 1997) describes a system divided into three parts: 1) a heat source which is made up of a relatively shallow magmatic chamber; 2) one or more aquifers located above the chamber; the degassing magma supplies fluids and heat to them; 3) an intensely fractured zone, sited above the uppermost aquifer and occupied by a pure vapor phase, which is produced through the boiling of the underlying aquifers.

The intense fumarolic activity has given origin to strong hydrothermal alteration of the original rocks (De Gennaro *et al.*, 1980) and to secondary deposits. In fact, the trachytic rocks of the floor and of the flanks of the volcano are bleached and corroded by the effluent vapours, with formation of gypsum, alum, kaolin and alunite (Valentino *et al.*, 1999). Moreover, sublimation of the emitted gas causes deposition of sulphur, arsenic sulphide (realgar), ammonium chloride (sal ammoniac), mercury sulphide and antimony sulphide.

4. Atmospheric correction

The spectral radiance L_D received by a remote sensor in the thermal infrared can be expressed as

$$L_D(\lambda) = [\varepsilon(\lambda) \cdot B(\lambda, T_s) + (1 - \varepsilon(\lambda)) \cdot L_d(\lambda)] \cdot \\ \cdot \tau(\lambda) + L_u(\lambda) \qquad (4.1)$$

where L_u is the upward atmospheric radiance, L_d is the downward atmospheric radiance, T_s is the surface kinetic temperature, ε is the surface emissivity, τ is the atmospheric transmittance between the surface and the sensor, and $B(T_s)$ is the Plank function.

In order to calculate the radiance emitted by the surface ($L(\lambda, T_s) = \varepsilon(\lambda) \cdot B(\lambda, T_s)$), remote sensing data must be corrected for atmospheric effects. To estimate the atmospheric radiative contributions (L_u, L_d and τ), we used the MODTRAN 3.5 radiative transfer code (Berk *et al.*, 1989), giving as input the atmospheric profiles measured during the field campaign. The obtained values were convolved with the sensor response functions of the six thermal infrared channels (fig. 4).

The atmospheric terms were estimated for 20 different optical paths corresponding to view angle increments of ≈3° with respect to the nadir. Lower angle increments result in negligi-
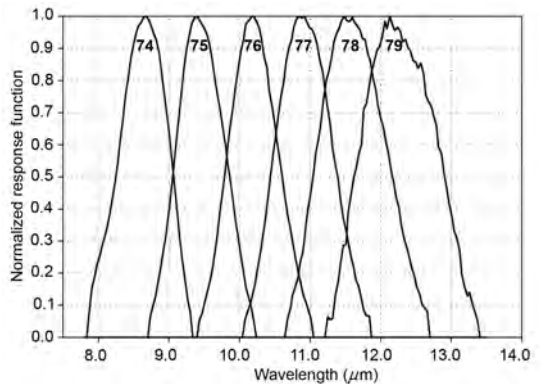

Fig. 4. Response functions of the DAIS thermal infrared channels.

ble variations. The different sets of atmospheric terms were used to apply separate corrections on image stripes corresponding to the view angle increments and parallel to the image axis.

5. Evaluation of surface temperature and emissivity

The spectral radiance emitted by a body having a kinetic temperature T_s can be expressed as a function of the spectral emissivity ε of its surface and of the Plank function B

$$L(\lambda, T_s) = \varepsilon(\lambda) \cdot B(\lambda, T_s). \qquad (5.1)$$

If the radiance L is measured at N wavelengths λ, the relation is expressed by a system of N equations with $N+1$ unknowns, *i.e.* the N values of spectral emissivity and the temperature.

This makes it difficult to estimate surface temperature and emissivity from remote sensing data because the equation system is not closed. In the literature, different «non-exact» solutions are given to this problem, called «temperature and emissivity separation» (Gillespie *et al.*, 1998; Li *et al.*, 1999).

In our work we applied the well established method of the Emissivity Spectrum Normalization (ESN) (Gillespie, 1985; Realmuto, 1990). According to this method, emissivity is normalized to a value ε_{max} corresponding to the maximum value expected in the scene. This method demonstrated good capability to maintain the spectrum shape, that is the most important feature in applications of spectral analysis and mapping.

Assuming $\varepsilon = \varepsilon_{max}$ for each value of λ, the inversion of eq. (5.1) gives N values of temperature; the highest of them is assumed to be the estimate of the kinetic temperature T_s. With this value, and using the Plank equation, the black body spectral radiance of the pixel is calculated. Finally, the emissivity is obtained dividing the surface radiance measured by the sensor by the calculated black body radiance, at each wavelength. Repeating this procedure for every pixel, temperature and spectral emissivity maps are obtained. In this study we assumed a value $\varepsilon_{max} = 0.97$ on the basis of the spectral libraries data (Salisbury *et al.*,

1991; Salisbury and D'Aria, 1992) available for the typical minerals of the Solfatara crater.

6. Selection of the areas of interest

The atmospheric correction and the temperature and emissivity estimation were performed on an image window chosen in the Solfatara crater.

Urban areas adjacent to the Solfatara were excluded applying a suitable mask cropped on the original image. On these areas reliable estimates of surface temperature and spectral emissivity cannot be obtained by the *ESN* method due to the urban covers extreme heterogeneity that makes it impossible to define a value of ε_{max} valid for the whole image. Moreover, the estimated surface temperature can be considered validated only inside the crater, where the *in situ* temperature was measured during the ground campaign.

In the images showing the elaboration results (figs. 5, 6 and 8), non-processed areas were masked with an image of a thermal channel to preserve topographic reference.

A further selection was applied to identify the areas of interest for geo-mineralogical interpretation: the vegetation cover was excluded with a mask based on the Normalized Difference Vegetation Index (NDVI). The data of two channels of visible (red) and near infrared are transformed by NDVI in a new image related to the green biomass using a spectral property of green vegetation: the sharp increase in reflectance between 0.65 and 0.80 μm (red edge).

The NDVI image was obtained using the DAIS channels 10 (0.659 μm) and 18 (0.802 μm); it was then converted in a mask by selecting a threshold value between vegetated and non vegetated pixels.

7. Results

Figure 5 shows the quantitative map of surface kinetic temperature. Values retrieved in the ground measurement sites (fig. 1) were extracted from this map and compared with ground temperatures: the comparison revealed a good agreement, as shown in table II.
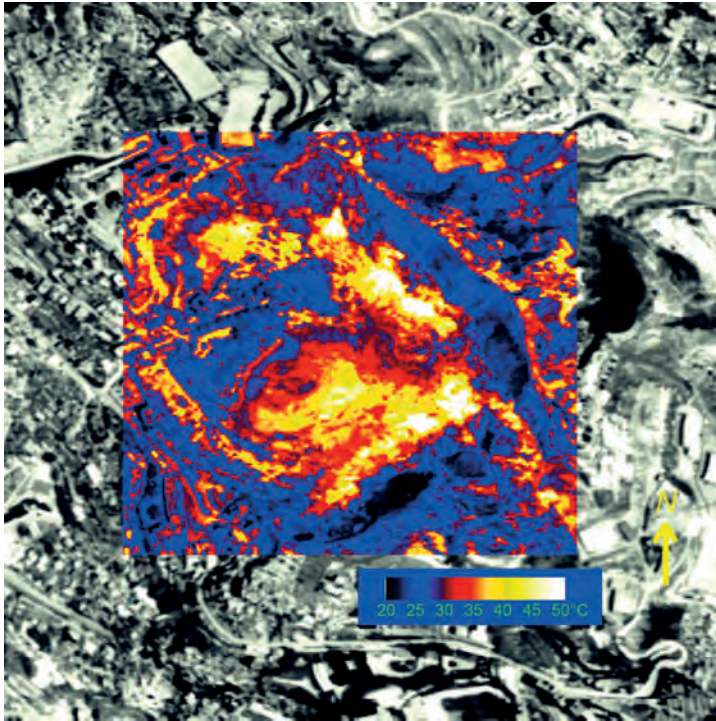
Fig. 5. Surface temperature map of the Solfatara crater retrieved by DAIS data.

Table II. Comparison between ground measured temperature and image retrieved temperature at the sites shown in fig. 1.

Site	Measurement start/end (local time)	Ground temperature (°C)	Image retrieved temperature (°C)
Fumarole; dark grey soil (1FF)	11.10/11.15	45.18±4.31	44.2
Central area (1CA)	11.20/11.25	44.91±2.60	42.7
White tuffs (1WT)	11.30/11.31	37.18±0.24	36.9
Campground (2CG)	10.40/10.43	44.54±1.87	42.7
Dry grass (2DG)	10.45/10.50	54.71±3.31	50.7
Tuffs (2T)	10.55/11.00	42.32±2.32	40.0

The six images of spectral emissivity allowed us to discriminate different surface covers on the basis of their spectral characteristics. An example is reported in fig. 6, where an RGB composition of spectral emissivity calculated in channels 78, 76 and 74 is reported.

By analyzing the emissivity images and the corresponding spectra, we could discriminate 6 main units, whose spectra differ strongly from each other. Fumarolic fields are well separable since they have a very distinctive spectral pattern, and materials with different emissive prop-
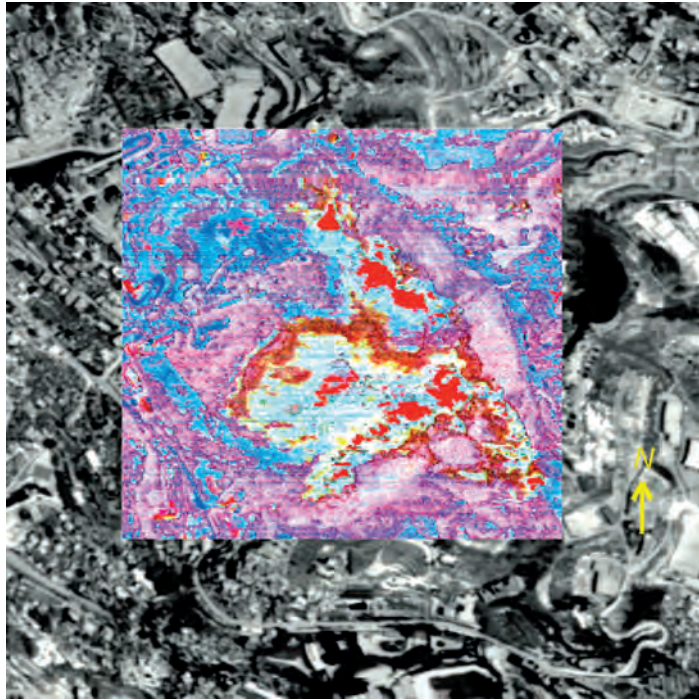
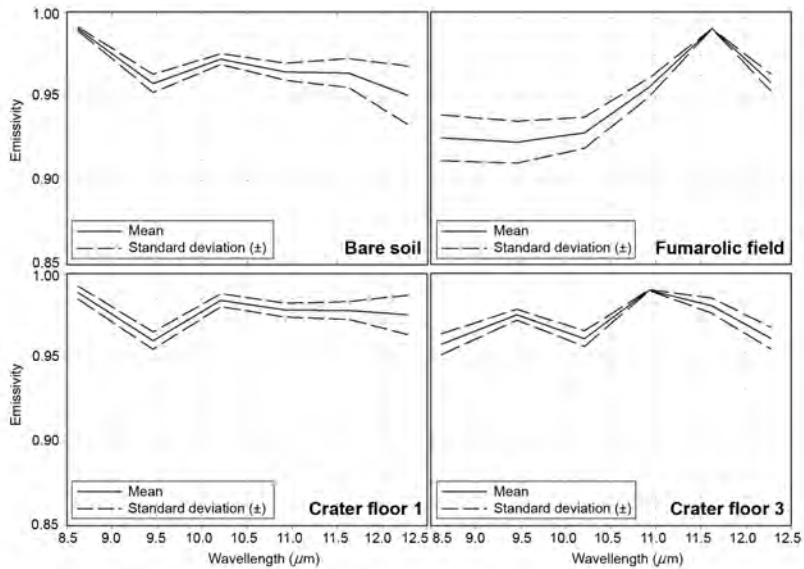**Fig. 6.** Spectral emissivity image in DAIS channels 78-76-74 (RGB).

Fig. 7. Emissivity spectra retrieved from the DAIS data. Average values were calculated on regions of interest selected on the main surface units.
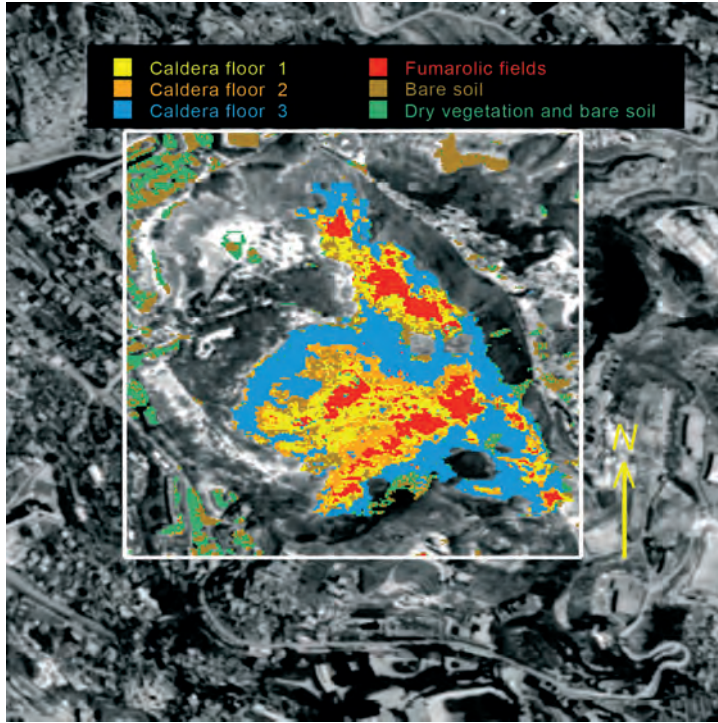
Fig. 8. Map of the main geo-mineralogical units outcropping at the Solfatara crater.

erties are recognizable, probably corresponding to different degrees of hydrothermal alteration of the surface and to depositions from fumarolic gases. An example of the emissivity spectra of the separated units is reported in fig. 7.

Spectral information retrieved from the emissivity images was used to produce a map of the main geo-mineralogical units outcropping at the Solfatara crater, applying the Spectral Angle Mapper (SAM) technique (Kruse *et al.*, 1993) (fig. 8). SAM is a physically-based spectral classification that uses an *n*-dimensional angle to match pixels to reference spectra (end-members). The algorithm determines the spectral similarity between two spectra by calculating the angle between the spectra, treating them as vectors in a space with dimensions equal to the number of bands (RSI, 2002). Non-processed areas and zones covered by vegetation were previously masked as already de-

scribed. Pure spectra required by this technique were obtained averaging spectra of small groups of pixels, selected on the image on the basis of information drawn from field survey and spectral analysis (fig. 7).

The six units detected were only separated but not yet identified at this stage of the work: to do this, representative emissivity measurements are needed to be compared with image spectra. Emissivity spectra of surface materials are strongly influenced by various factors (Salisbury and D'Aria, 1992) such as granulometry, temperature, compaction level, water content. In a remote sensing scene, pixel spectra are also influenced by local un-homogeneities of the deposits. For these reasons, a direct comparison between image spectra and reference spectra of minerals from public spectral libraries is not feasible; field measurements of spectral emissivity are required to perform reliable comparisons.

8. Conclusions and future work

DAIS thermal infrared data were used to retrieve surface temperature ad spectral emissivity maps of the Solfatara crater. Our results confirm DAIS capability to provide valuable volcanological information based on the thermal infrared properties of materials. The quantitative temperature map of the area we obtained allows us to locate thermal anomalies corresponding to active fumaroles and to characterize their thermal properties. The spectral emissivity image allows the mapping of the main geo-mineralogical units on the basis of their spectral properties. This thematic map points out that six thermal infrared channels are sufficient to detect and separate not only different surface covers but also similar materials whose differences are mainly related to their alteration degree.

In order to complete the image interpretation and perform the automatic identification of the classes, field acquisition of emissivity spectra is planned. Spectral emissivity will be measured with a portable FTIR (Fourier Transform Infra-Red) spectrometer (Design & Prototypes LTD) working in the 2-16 μm spectral range with a spectral resolution between 2 and 16 cm^{-1}. Sampled materials will be analyzed in the laboratory to retrieve chemical and mineralogical features corresponding to the field collected spectra.

REFERENCES

BERK, A., L.S. BERNSTEIN and D.C. ROBERTSON (1989): MODTRAN: a moderate resolution model for LOW-TRAN-7, *AF-GL Technical Report GL-TR-89-0122* (Air Force, Hanscom, MA, U.S.A.).

BERRINO, G., G. CORRADO, G. LUONGO and B. TORO (1984): Ground deformation and gravity changes accompanying the 1982 Pozzuoli uplift, *Bull. Volcanol.*, **47** (2), 187-200.

CHIODINI, G., R. CIONI, G. MAGRO, I. MARINI, C. PANICHI, B. RACO and M. RUSSO (1997): Chemical and isotopic variations of Bocca Grande Fumarole (Solfatara volcano, Phlegraean Fields), *Acta Vulcanol.*, **8** (2), 228-232.

CORRADO, G., I. GUERRA, A. LO BASCIO, G. LUONGO and R. RAMPOLDI (1976): Inflation and microearthquake activity of Phlegraean Fields, Italy, *Bull. Volcanol.*, **40** (3), 169-188.

DE GENNARO, M., E. FRANCO and D. STANZIONE (1980): Le alterazioni ad opera di fluidi termali alla solfatara di Pozzuoli (Napoli), *Mineral. Geochim.*, **49**, 5-22.

DI VITO, M., L. LIRER, G. MASTROLORENZO, G. ROLANDI and R. SCANDONE (1985): *Volcanological Map of Campi Flegrei* (Min. Prot. Civ., Università degli Studi di Napoli).

DI VITO, M., L. LIRER, G. MASTROLORENZO and G. ROLANDI (1987): The 1538 Monte Nuovo eruption (Campi Flegrei, Italy), *Bull. Volcanol.*, **49**, 608-615.

DI VITO, M.A., R. ISAIA, G. ORSI, J. SOUTHON, S. DE VITA, M. D'ANTONIO, L. PAPPALARDO and M. PIOCHI (1999): Volcanism and deformation in the past 12 ka at the Campi Flegrei caldera (Italy), *J. Volcanol. Geotherm. Res.*, **91**, 221-246.

GILLESPIE, A.R. (1985): Lithologic mapping of silicate rocks using TIMS, in *The TIMS Data User's Workshop*, *Jet Propulsion Laboratory Publ. 86-38*, 29-44.

GILLESPIE, A., S. ROKUGAWA, T. MATSUNAGA, J.S. COTHERN, S. HOOK and A. KAHLE (1998): A temperature and emissivity separation algorithm for Advanced Spaceborne Thermal Emission and Reflection Radiometer (ASTER) images, *IEEE Trans. Geosci. Remote Sensing*, **36** (4),1113-1126.

KRUSE, F. A., A.B. LEFKOFF, J.B. BOARDMAN, K.B. HEIDEBRECHT, A.T. SHAPIRO, P.J. BARLOON and A.F.H. GOETZ (1993): The Spectral Image Processing System (SIPS) – Interactive visualization and analysis of imaging spectrometer data, *Remote Sensing Environ.*, **44**, 145-163.

LI, Z., F. BECKER, M. STOLL and Z. WAN (1999): Evaluation of six methods for extracting relative emissivity spectra from thermal infrared images, *Remote Sensing Environ.*, **69**, 197-214.

LIRER, L., G. LUONGO and R. SCANDONE (1987): On the volcanological evolution of Campi Flegrei, *EOS, Trans. Am. Geophys. Un.*, **68**, 226-234.

REALMUTO, V.J. (1990): Separating the effects of temperature and emissivity: emissivity spectrum normalization, in *Proceedings of the 2nd TIMS Workshop, JPL Publ. 90-55*.

RSI (2002): *ENVI 3.6 User's guide* (Research Systems, Inc.).

SALISBURY, J.W. and D.M. D'ARIA (1992): Emissivity of terrestrial materials in the 8-14 mm atmospheric window, *Remote Sensing Environ.*, **65**, 83-106.

SALISBURY, J.W., L.S. WALTER, N. VERGO and D.M. D'ARIA (1991): *Infrared (2.1-25 μm) Spectra of Minerals* (Johns Hopkins University Press), pp. 294.

SCANDONE, R. (1997): *Campi Flegrei* (on line: http://vulcan.fis.uniroma3.it/campi_flegrei/geol.gif/, modified after Di Vito *et al.*, 1985).

SCANDONE, R., F. BELLUCCI, L. LIRER and G. ROLANDI (1991): The structure of the Campanian Plain and the activity of Neapolitan Volcanoes, *J. Volcanol. Geotherm. Res.*, **48** (1-2), 1-31.

VALENTINO, G.M., G. CORTECCI, E. FRANCO and D. STANZIONE (1999): Chemical and isotopic compositions of minerals and waters from the Campi Flegrei volcanic system, Naples, Italy, *J. Volcanol. Geotherm. Res.*, **91**, 329-344.